Electronic Supplementary Material (ESI) for RSC Advances.

Electronic Supplementary Information

Supramolecular Cu(II) nanoparticles supported on a functionalized chitosan containing urea and thiourea bridges as a recoverable nanocatalyst for efficient synthesis of 1*H*-tetrazoles

Shirin Bondarian, Mohammad G. Dekamin*, Ehsan Valiey, M. Reza Naimi-Jamal

[a]*Pharmaceutical and Heterocyclic Compounds Research Laboratory Department of Chemistry Iran University of Science and Technology. Email: mdekamin@iust.ac.ir*

Graphical Abstract

Cu(II) nanoparticles supported on a functionalized chitosan containing urea and thiourea bridges as a recoverable nanocatalyst for efficient synthesis of 1*H*-tetrazoles

Shirin Bondarian, Mohammad G. Dekamin*, Ehsan Valiey, M. Reza Naimi-Jamal

A cost-effective and convenient method for supporting of Cu(II) nanoparticles (Cu NPs) on the chitosan containing urea and thiourea bridges backbone using toluene-2,4-diisocyanate (TDI) and pyromellitic dianhydride (PMDA) linkers was designed and characterized by applicable spectroscopic and analytical techniques. The heterogeneous low-loaded Cu(II) nanoparticles was successfully employed in the multicomponent cascade Knoevenagel condensation/click 1,3-dipolar cycloaddition in good to excellent yields with proper reusability.

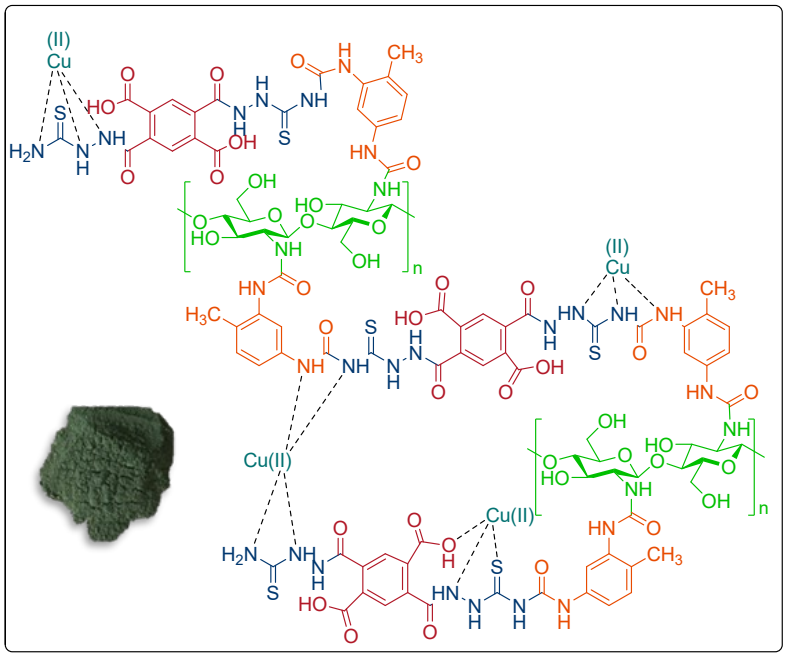

CS-TDI-PMDA-TS-Cu(II)

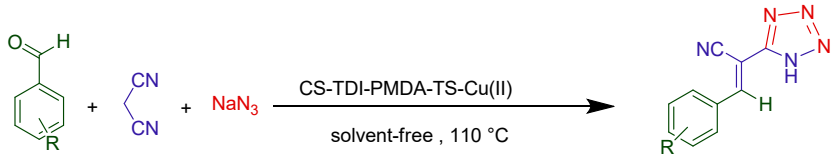

Catalyst Preparation:

The graphical procedure for the synthesis of the catalyst is shown in **Scheme S1.**

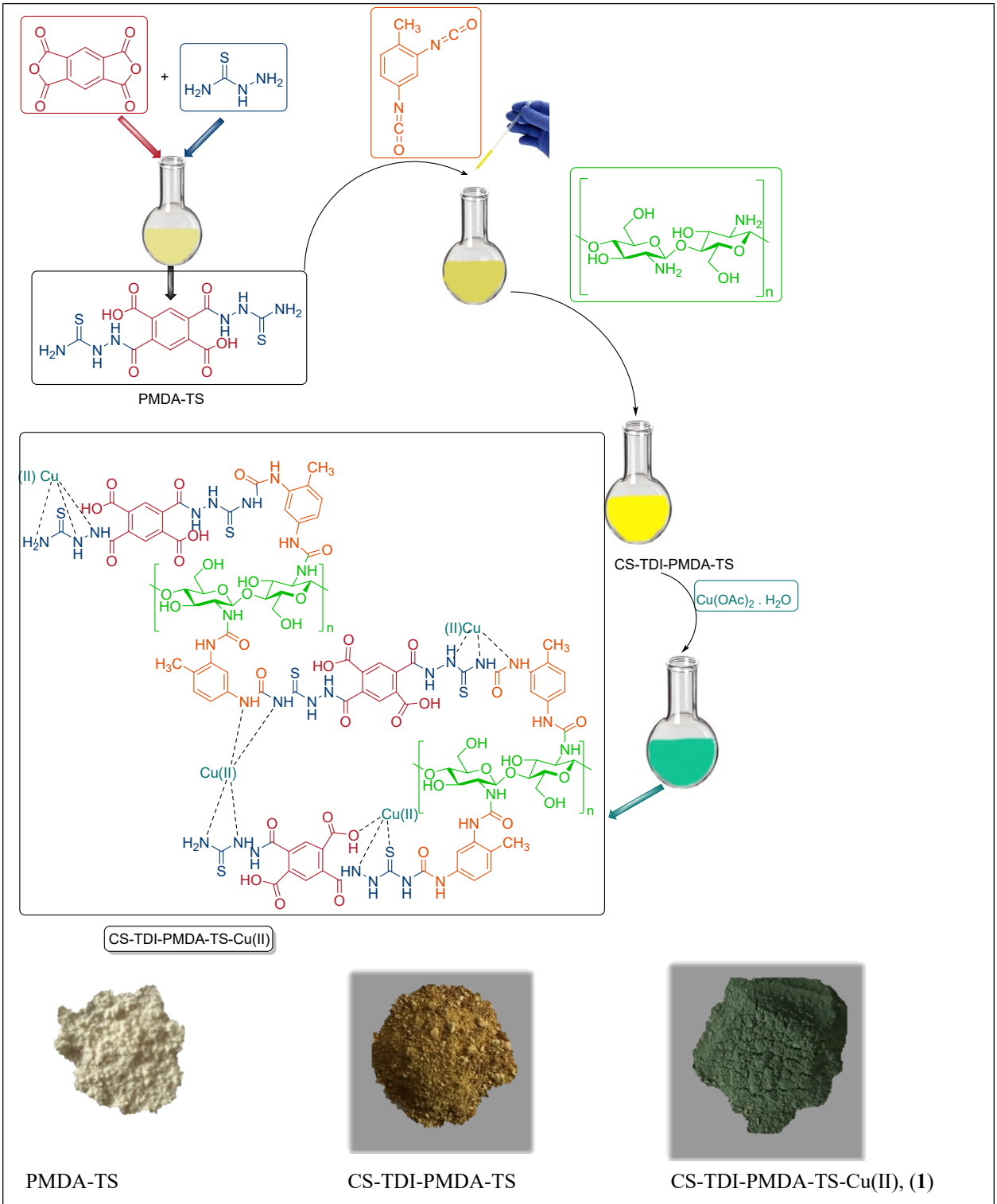

Scheme S1 Schematic representation of (CS-TDI-PMDA-TS-Cu(Ⅱ)) catalyst (1) preparation steps.

Model Reaction:

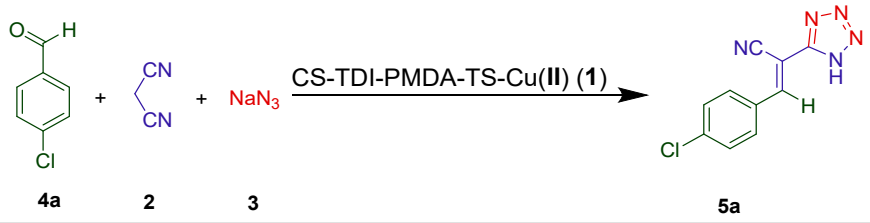

The model reaction for 5-substituted-1*H*-tetrazole derivatives catalyzed by catalyst **1**.

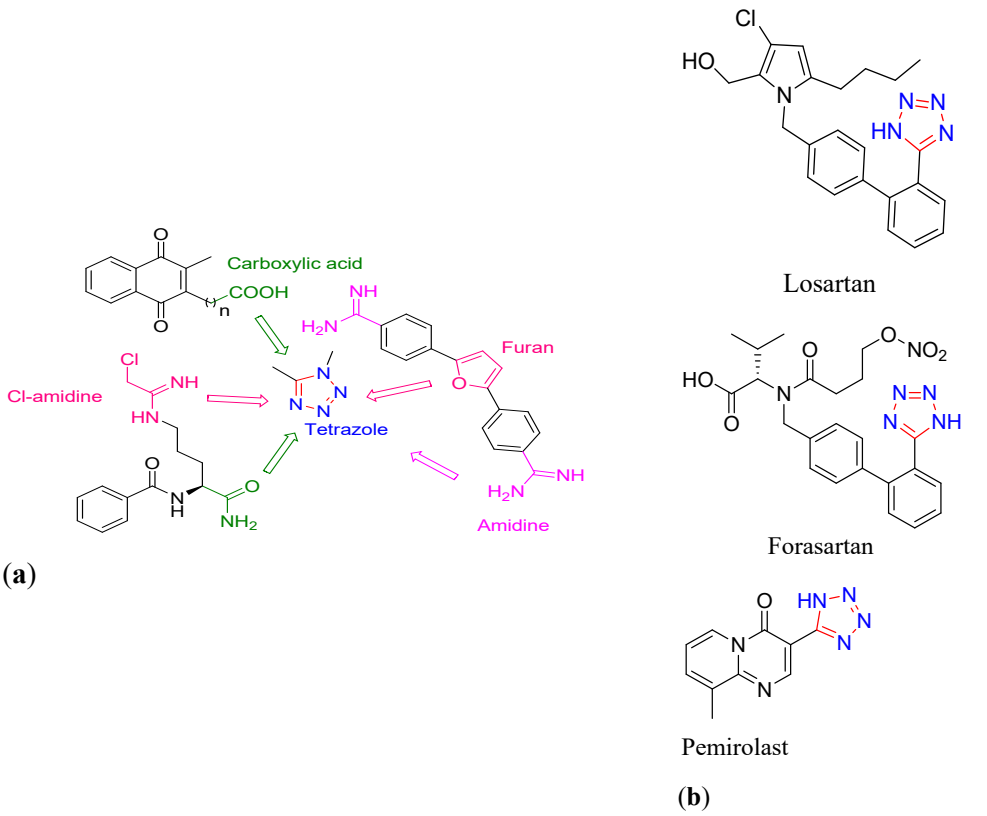

Fig. S1 (**a**) Tetrazole scaffold as bioisostere of the carboxylic group, Cl-amidine, or heterocyclic furan ring in medicinal chemistry; (**b**) Active pharmaceutical ingredients having tetrazole moiety: Losartan, Forasartan, and Pemirolast.

FTIR Spectrums:

The FTIR spectra from initiators are illustrated in (**Fig. S2**).

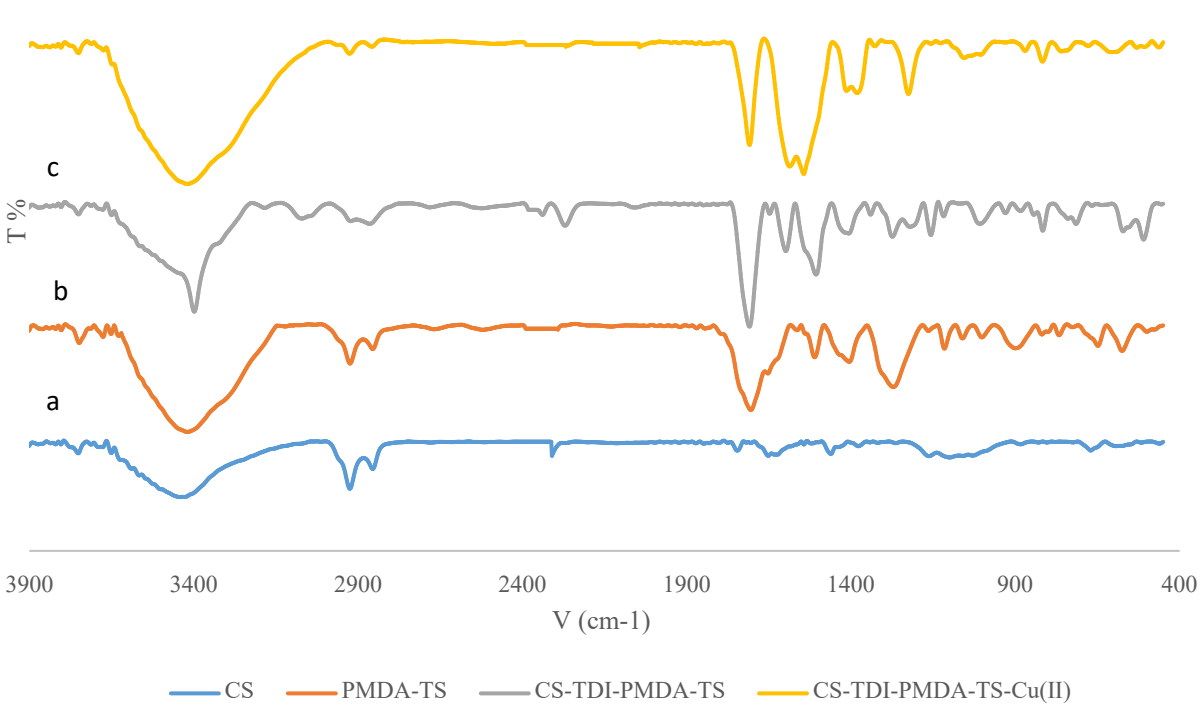

Fig. S2 FT-IR spectra of the commercial CS, PMDA-TS, CS-TDI-PMDA-TS, and the CS-TDI-PMDA-TS-Cu(Ⅱ) nanocomposite (**1**).

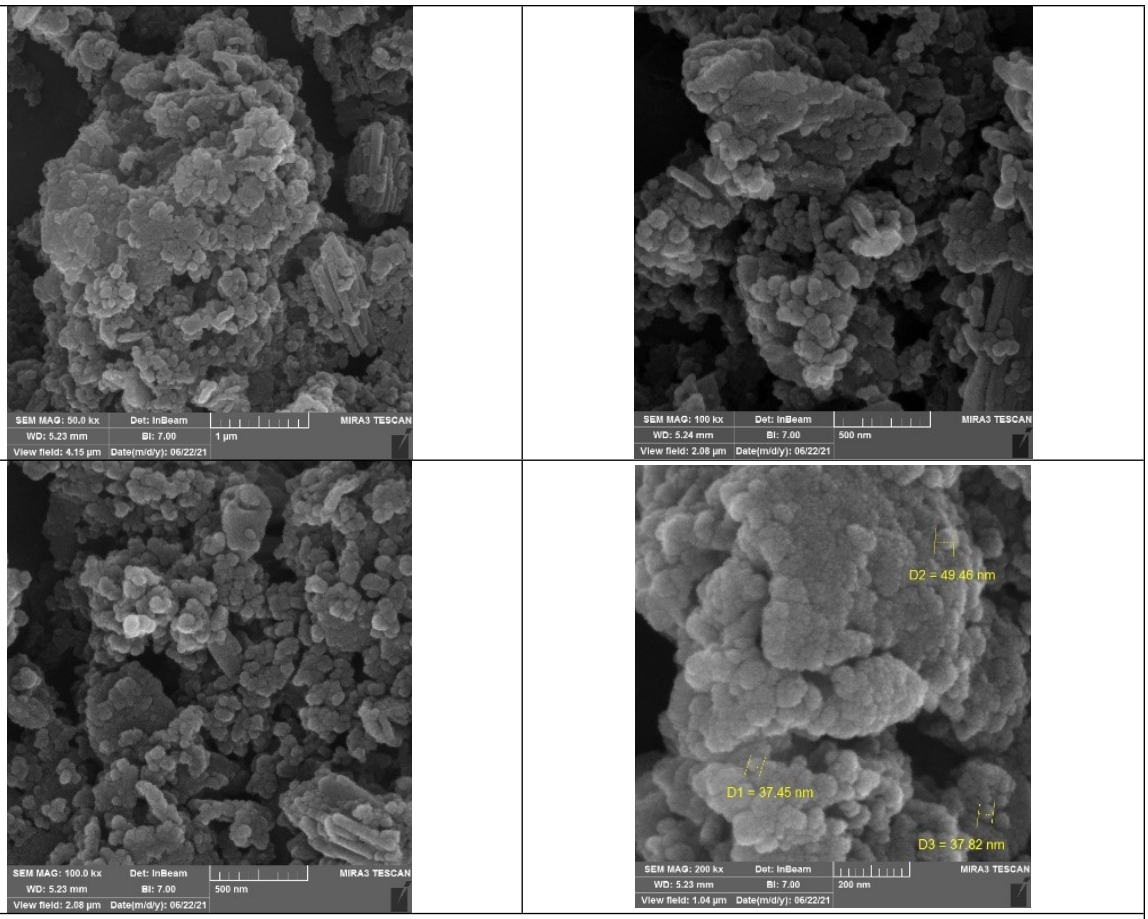

Fig. S3 FESEM images of the CS-TDI-PMDA-TS-Cu(Ⅱ) nanocomposite (**1**).

Fig. S4 TGA/DTA analysis of the CS-TDI-PMDA-TS-Cu(Ⅱ) nanomaterial (**1**).

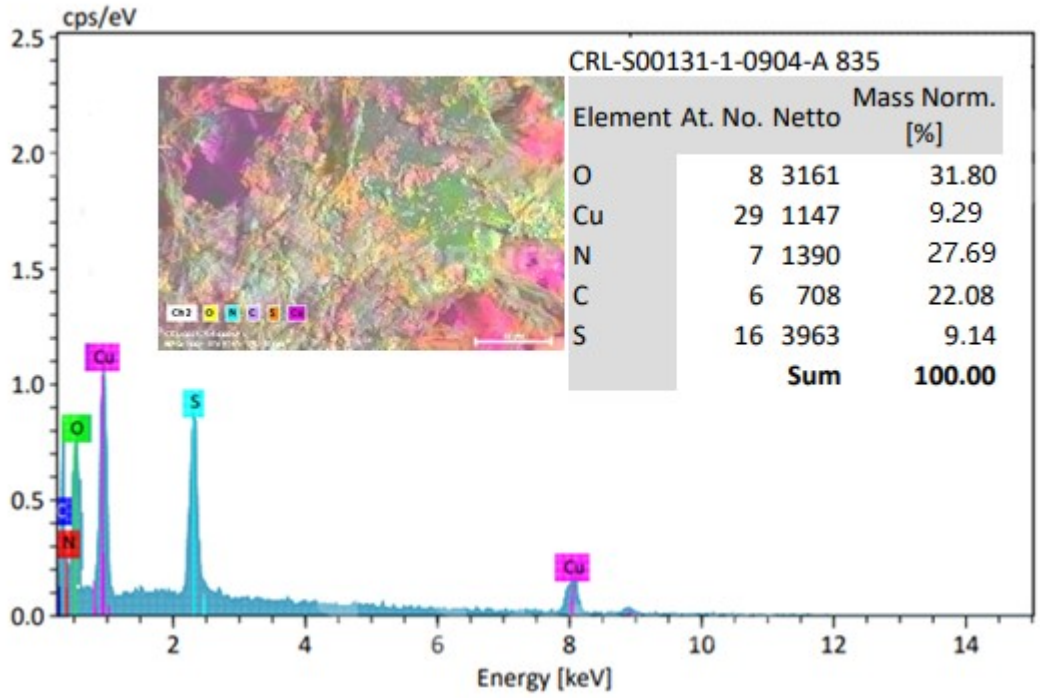

Fig. S5 The EDX spectrum of the CS-TDI-PMDA-TS-Cu(Ⅱ) nanocatalyst (**1**).

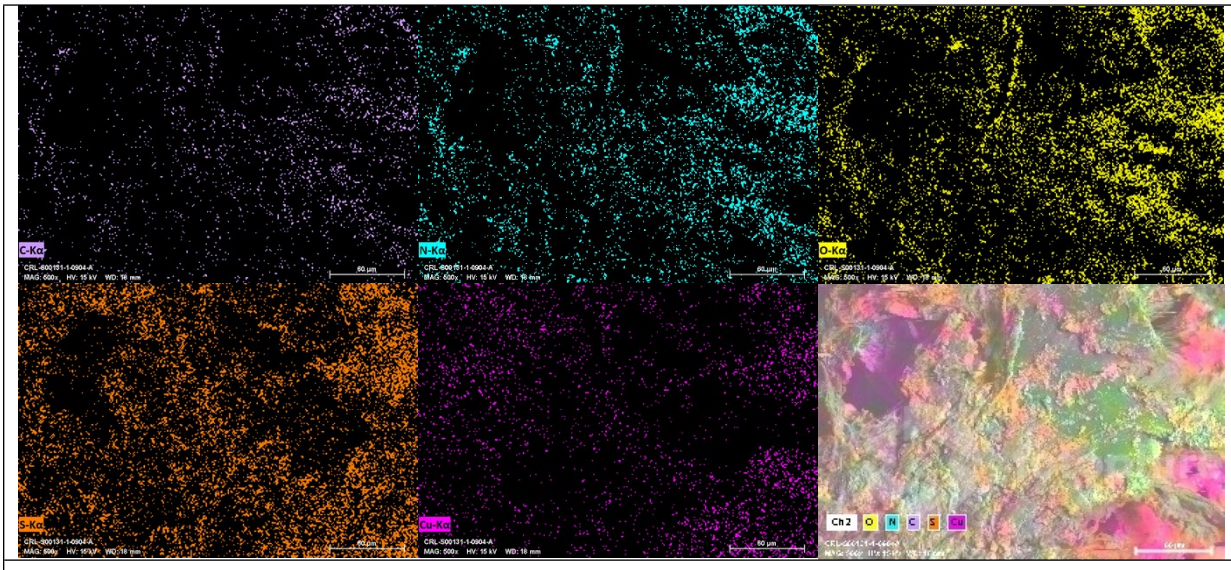

Fig. S6 Mapping of the CS-TDI-PMDA-TS-Cu(Ⅱ) nanocatalyst (**1**).

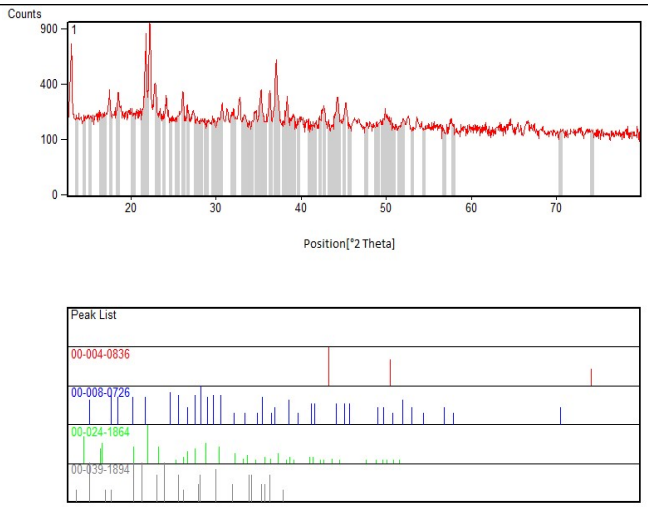

Fig. S7 The XRD pattern for CS-TDI-PMDA-TS-Cu(Ⅱ) nanocatalyst (**1**).

Table S1 Optimization of the conditions for 1*H*-tetrazole in the model reaction of malononitrile (**2**), NaN_3 (**3**), and 4-chlorobenzaldehyde (**4a**) under different conditions[a]

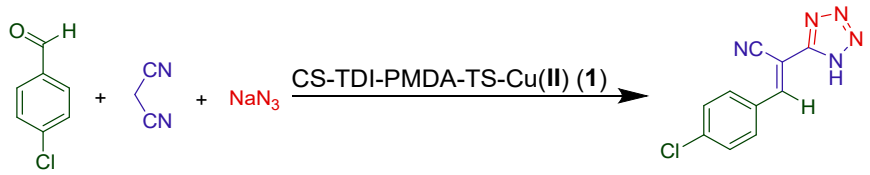

4a **2** **3** **5a**

Entry	Catalyst	Catalyst loading (mg)	Solvent	Temperature (°C)	Time (min)	yield[b] of (%) 5a
1	-	-	Solvent-Free	110	24 h	60
2	-	-	DMF	Reflux	20 h	50
3	CS-TDI-PMDA-TS-Cu(Ⅱ) (**1**)	10	Solvent-Free	110	30	65
4	CS-TDI-PMDA-TS-Cu(Ⅱ) (**1**)	15	Solvent-Free	110	30	80
5	**CS-TDI-PMDA-TS-Cu(Ⅱ) (1)**	**20**	**Solvent-Free**	**110**	**30**	**92**
6	CS-TDI-PMDA-TS-Cu(Ⅱ) (**1**)	40	Solvent-Free	110	45	94
7	CS-TDI-PMDA-TS-Cu(Ⅱ) (**1**)	20	EtOH	Reflux	60	80
8	CS-TDI-PMDA-TS-	20	CH_2Cl_2	Reflux	60	50

	Cu(Ⅱ) (**1**)					
9	CS-TDI-PMDA-TS-Cu(Ⅱ) (**1**)	20	H_2O	Reflux	60	87
10	CS-TDI-PMDA-TS-Cu(Ⅱ) (**1**)	20	DMF	Reflux	60	90
11	CS-TDI-PMDA-TS-Cu(Ⅱ) (**1**)	20	EtOAc	Reflux	60	55
12	CS-TDI-PMDA-TS-Cu(Ⅱ) (**1**)	20	Solvent-Free	120	50	93
13	CS-TDI-PMDA-TS-Cu(Ⅱ) (**1**)	20	Solvent-Free	100	70	90
14	CS-TDI-PMDA-TS-Cu(Ⅱ) (**1**)	20	Solvent-Free	80	110	60

[a] Reaction conditions: malononitrile (**2**,1.1 mmol), sodium azide (**3**,1.5 mmol), and 4-chlorobenzaldehyde (**4a**,1 mmol) in the presence of 20 mg CS-TDI-PMDA-TS-Cu(Ⅱ) nanocatalyst (**1**). [b] Isolated yield.

Table S2 Synthesis of 5-substituted-1*H*-tetrazole derivatives **5a_q** catalyzed by CS-TDI-PMDA-TS-Cu(Ⅱ) (**1**)[a].

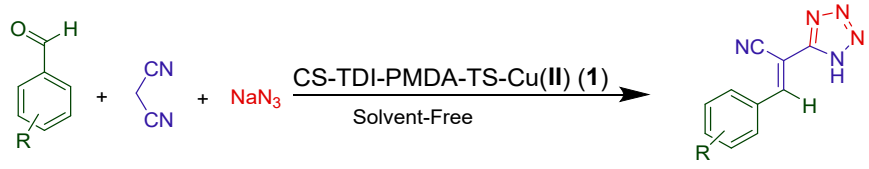

4a-q **2** **3** **5a-q**

Entry	Aldehyde (4)	Product (5)	Time (min)	Yield (%)[b]	M.p. (°C) [Obs.]	M.p. (°C) [Lit.]
1	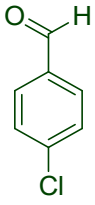 4a	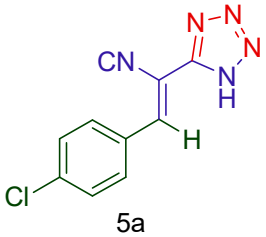 5a	**40**	**92**	**158-160**	**156-159**

2	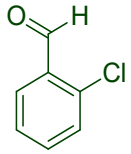 4b	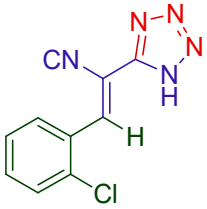 5b	**40**	**90**	**174-176**	**175-177**
3	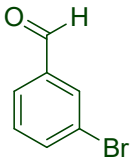 4c	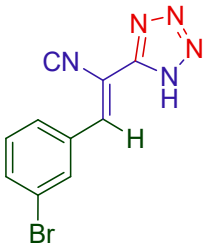 5c	**55**	**90**	**162-164**	**161-163**
4	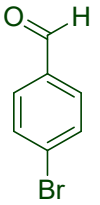 4d	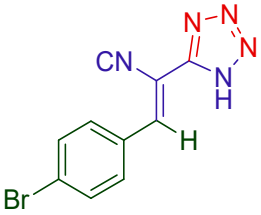 5d	**45**	**92**	**166-168**	**166-168**
5	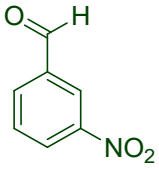 4e	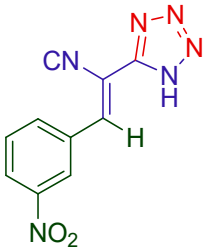 5e	**40**	**85**	**160-163**	**161-163**
6	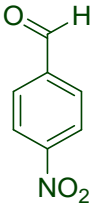 4f	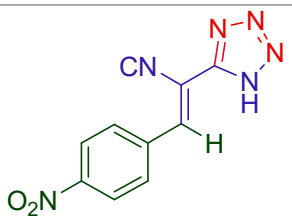 5f	**45**	**88**	**165-167**	**166-168**

7	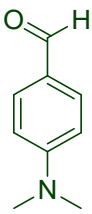 4g	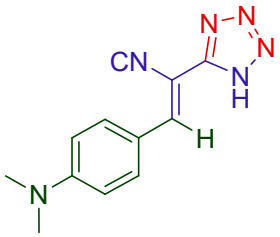 5g	**50**	**92**	**169-172**	**169-171**
8	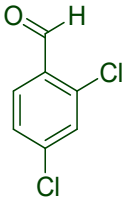 4h	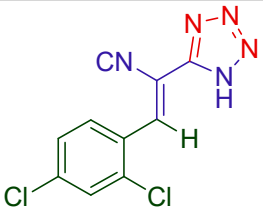 5h	**40**	**90**	**142-145**	**142-144**
9	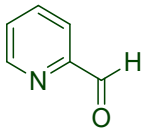 4i	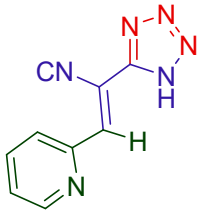 5i	**60**	**86**	**185-187**	**185-186**
10	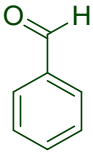 4j	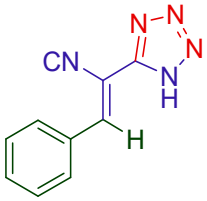 5j	**30**	**90**	**164-166**	**164-166**
11	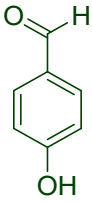 4k	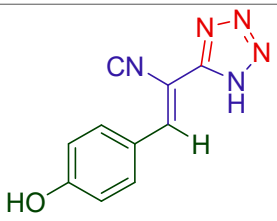 5k	**55**	**82**	**162-165**	**161-164**
12	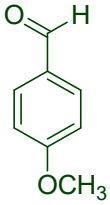 4l	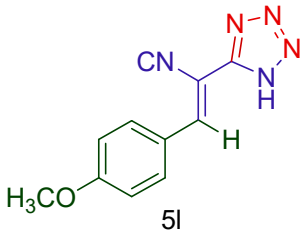 5l	**55**	**90**	**155-158**	**156-160**

13	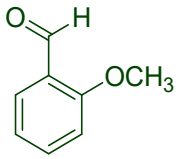 4m	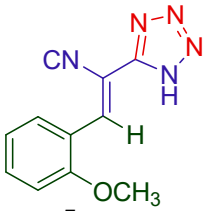 5m	**50**	**86**	**157-159**	**157-159**
14	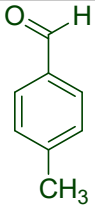 4n	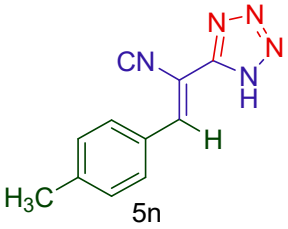 5n	**50**	**88**	**189-191**	**190-192**
15	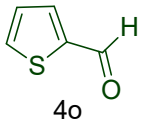 4o	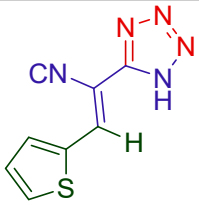 5o	**55**	**82**	**132-137**	**132-137**
16	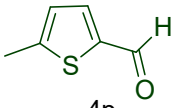 4p	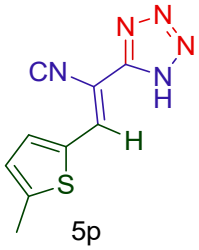 5p	**60**	**88**	**136-139**	**135-140**
17	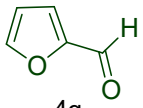 4q	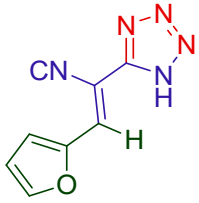 5q	**70**	**88**	**253-256**	**253-254**

[a] Reaction conditions: malononitrile (**2**, 1.1 mmol), sodium azide (**3**, 1.5 mmol), aryl aldehyde (**4a-q**, 1 mmol) in the presence of CS-TDI-PMDA-TS-Cu(Ⅱ) (**1**, 20 mg), 110 °C under solvent-free conditions.[b] Isolated yields.

Table S3 Comparison of the catalytic efficiency of the CS-TDI-PMDA-TS-Cu(Ⅱ) (1) with other catalytic systems**.**

Entry	Catalyst	Catalyst loading	Reaction Conditions	Time (hour)	Yield (%)	References
1	**CS-TDI-PMDA-TS-Cu (Ⅱ) (1)**	**20.0 mg**	**Solvent-Free/110 °C**	**30 min**	**92**	**Present work**
2	Nano-Fe_3O_4	20 mol%	Solvent-Free/80 °C	4.5	90	[108]

3	Fe_3O_4@fibroin-SO_3H	10 mol%	Solvent-Free/100 °C	2	86	113
4	Fe_3O_4-CNT-SO_3H nanocomposite	20.0 mg	Solvent-Free/80 °C	2.5	90	114
5	NiO nanoparticls	4.5 mg	DMF/70 °C	6	90	115
6	NH–Cu(Ⅱ)@MNP	20.0 mg	EtOH/80 °C	5	92	116
7	Zn (Mettalic)	130.7 mg	H_2O/50 °C	3	68	117
8	$(CuOTf)_2.C_6H_6$	36.2 mg	Toluene/r.t.	7	81	118
9	$Fe(OAc)_2$	17.4 mg	DMF/H_2O (9:1) 80 °C	24	89	119
10	OPNSA	45.4 mg	Solvent-Free/100 °C	10	80	120

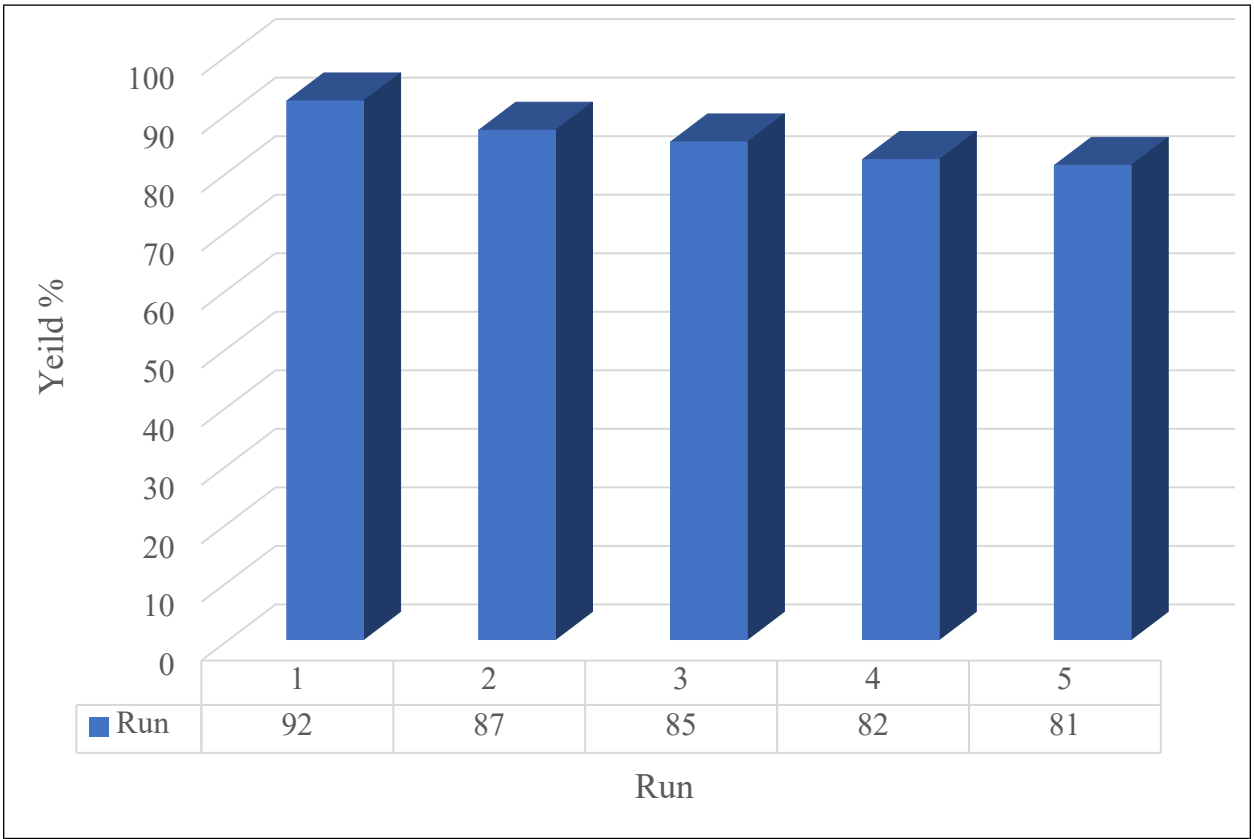

Fig. S8 Reusability data for the CS-TDI-PMDA-TS-Cu(Ⅱ) nanocatalyst (**1**) in the synthesis of **5a.**

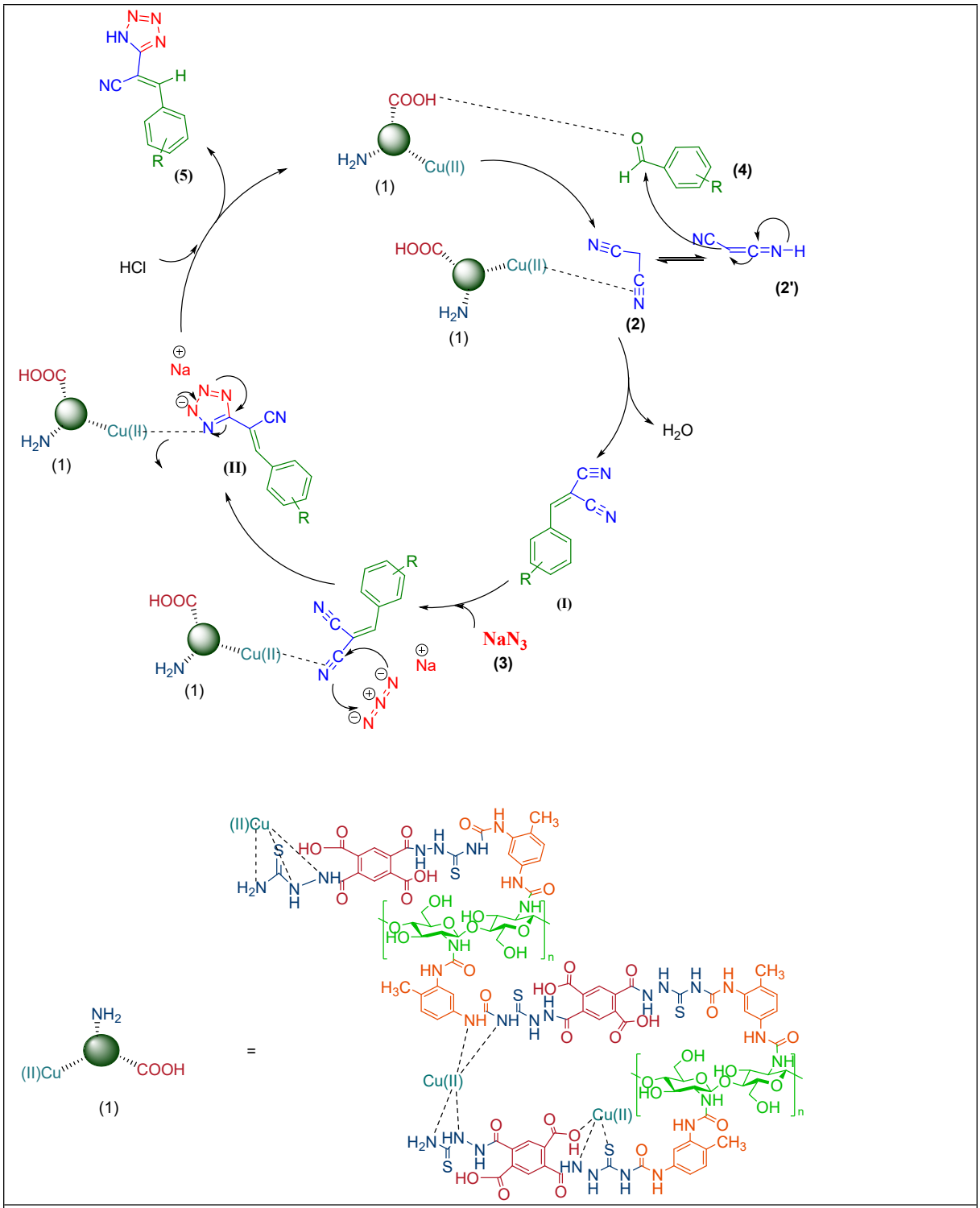

Scheme S2 The proposed mechanism for the synthesis of tetrazole derivatives catalyzed by the heterogeneous supramolecular CS-TDI-PMDA-TS-Cu(II) nanocatalyst (**1**).

Spectral data of the selected products

(*E*)-3-(2-chlorophenyl)-2-(1*H*-tetrazole-5-yl) acrylonitrile (5b):

Cream solid powder; Mp: 174-176 °C; FT-IR (KBr) v: 3241, 3025, 2207, 1573, 1475, 973, 824, 672 cm^{-1}; ^{1}H NMR (500 MHz, DMSO-d_6): δ (ppm) 7.55-7.57 (m, 2H), 7.65-7.67 (d, *J* = 8.4 Hz, 1H), 8.10-8.11 (d, *J* = 6.3 Hz, 1H), 8.42 (s, 1H, CH), 13.19 (s, 1H, NH).

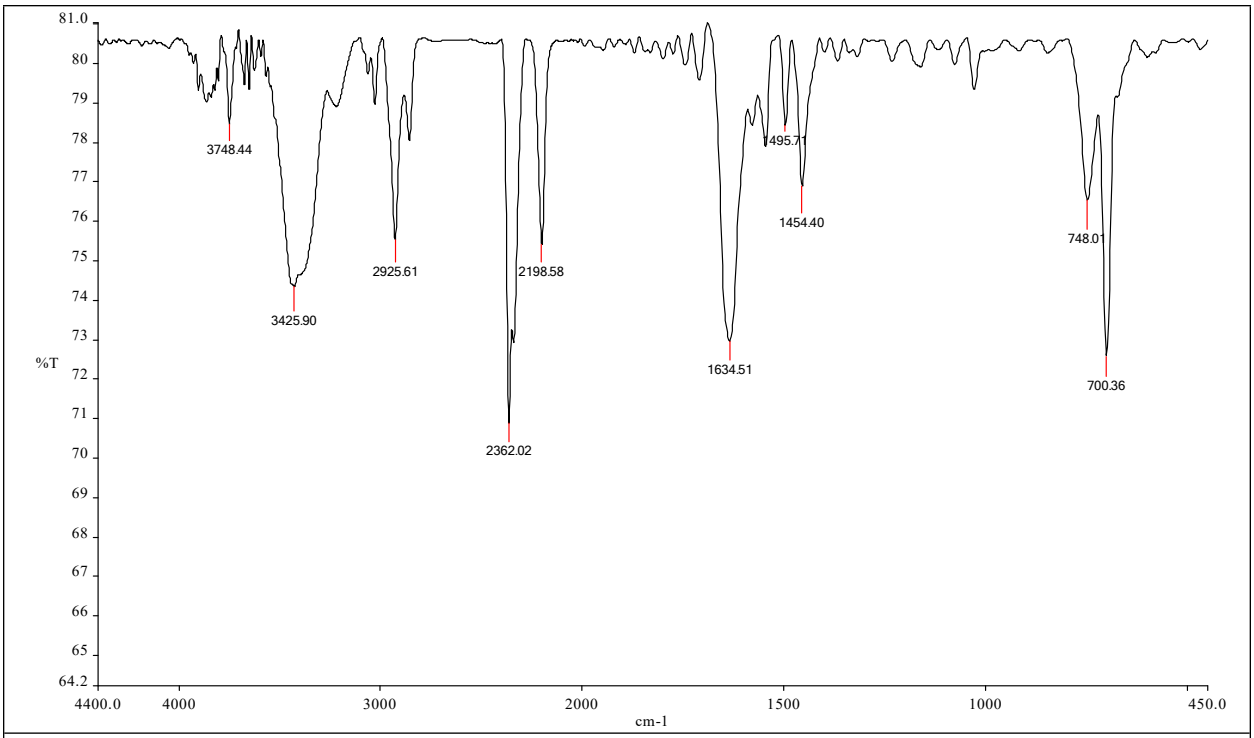

Fig. S9 FT-IR spectrum *of* (*E*)-3-(2-chlorophenyl)-2-(1*H*-tetrazole-5-yl) acrylonitrile (**5b**).

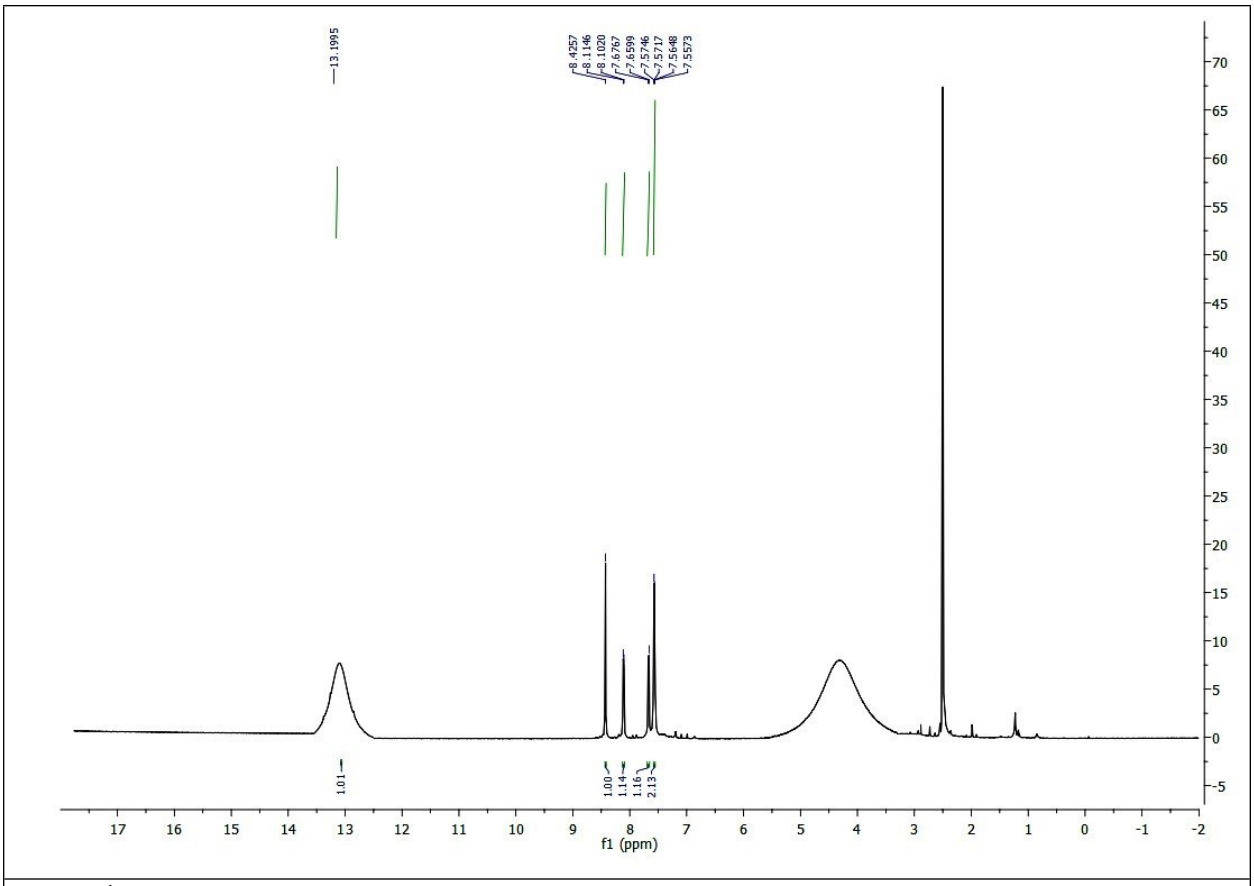

Fig. S10 ^{1}H NMR spectrum *of* (*E*)-3-(2-chlorophenyl)-2-(1*H*-tetrazole-5-yl) acrylonitrile (**5b**).

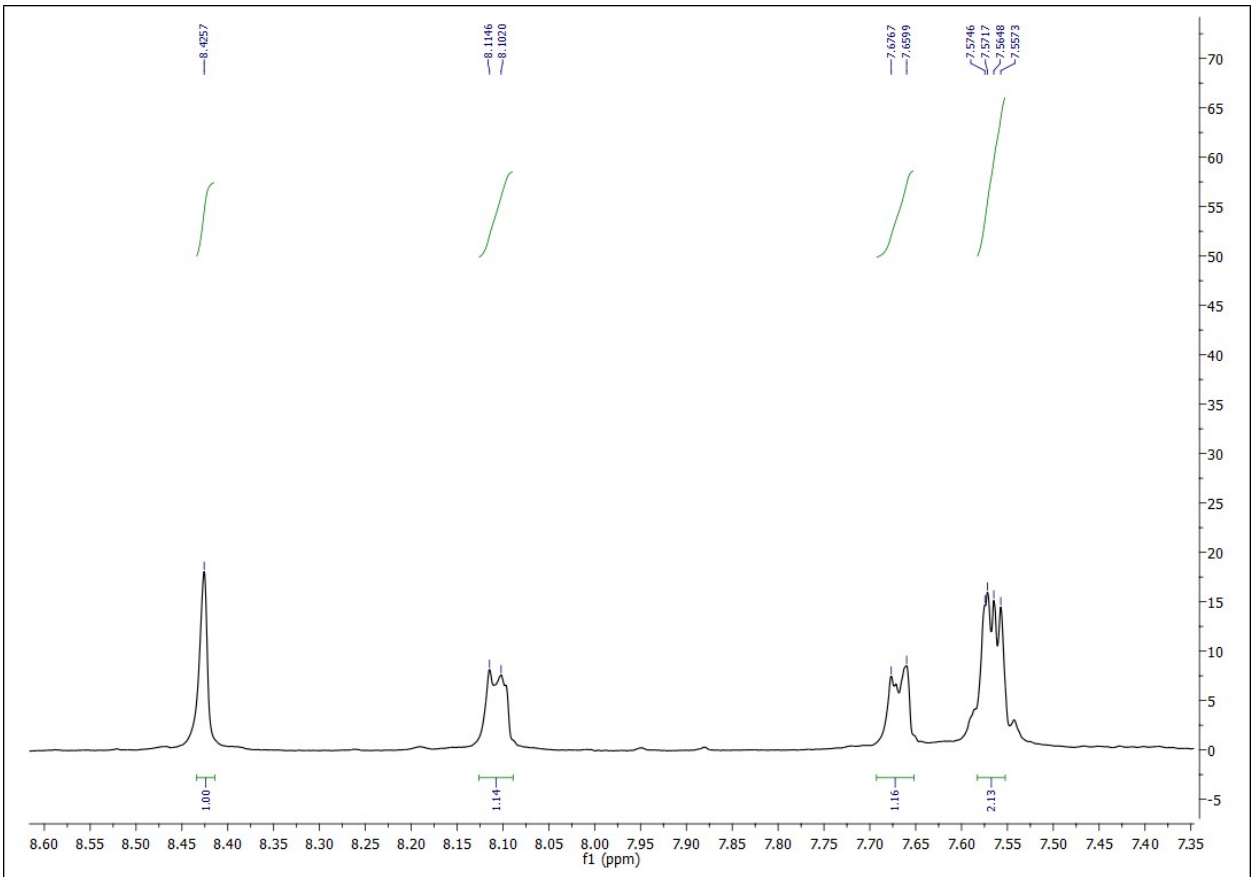

Fig. S11 Expanded ^{1}H NMR spectrum *of* (*E*)-3-(2-chlorophenyl)-2-(1*H*-tetrazole-5-yl) acrylonitrile (**5b**).

(*E*)-3-(4-methoxyphenyl)-2-(1*H*-tetrazole-5-yl) acrylonitrile (5l):
Pale yellow powder; Mp: 155-158 °C; FT-IR (KBr) v: 3148, 2256, 1573, 1416, 1118, 930, 810, 681, 649 cm^{-1}; ^{1}H NMR (500 MHz, DMSO-d_6): δ (ppm) 7.13-7.14 (d, *J* = 8.3 Hz, 2H), 8.00-8.02 (d, *J* = 8.3 Hz, 2H), 8.27 (s, 1H, CH), 13.40 (s, 1H, NH).

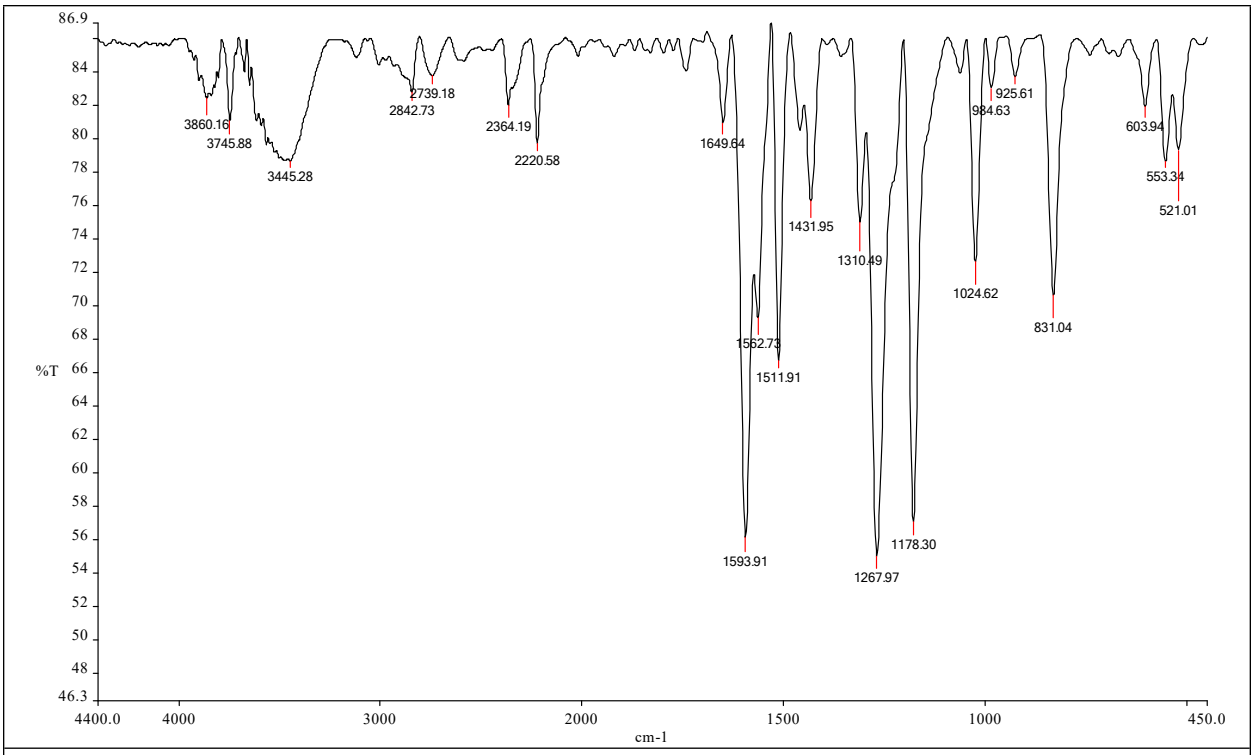

Fig. S12 FT-IR spectrum *of* (*E*)-3-(4-methoxyphenyl)-2-(1*H*-tetrazole-5-yl) acrylonitrile (**5l**).

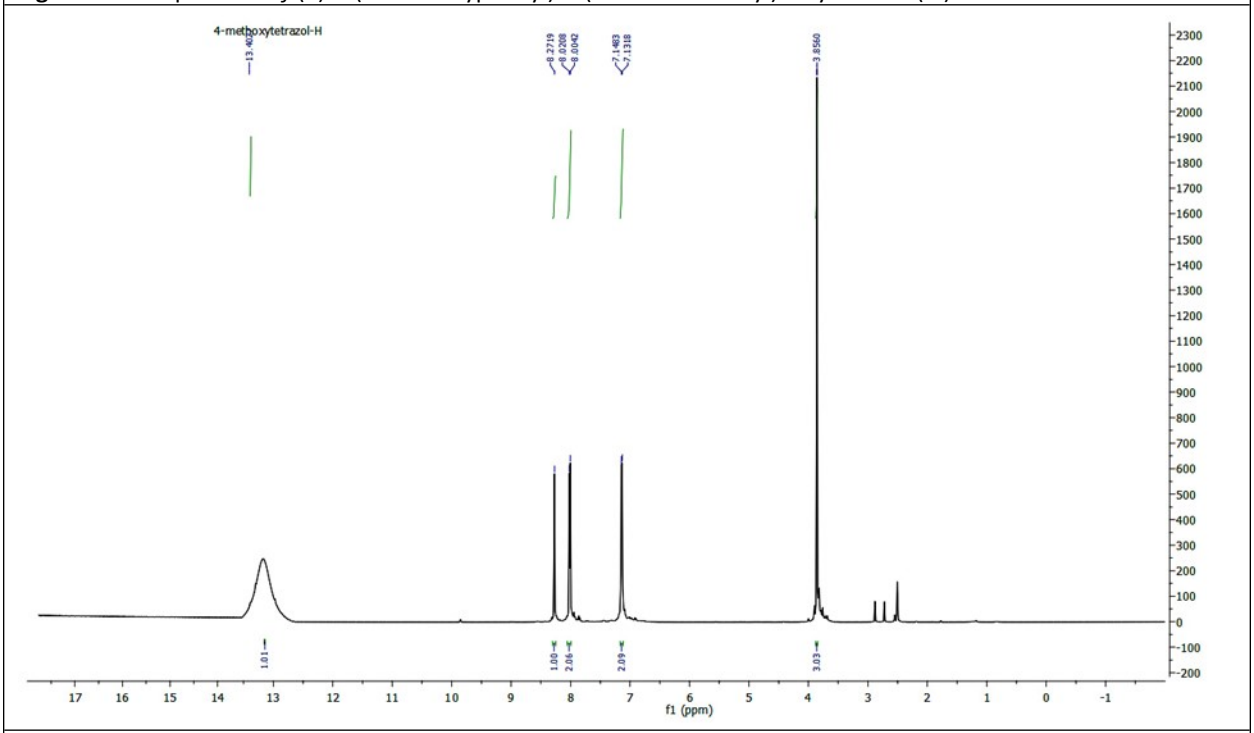

Fig. S13 ^{1}H NMR spectrum of (*E*)-3-(4-methoxyphenyl)-2-(1*H*-tetrazole-5-yl) acrylonitrile (**5l**).

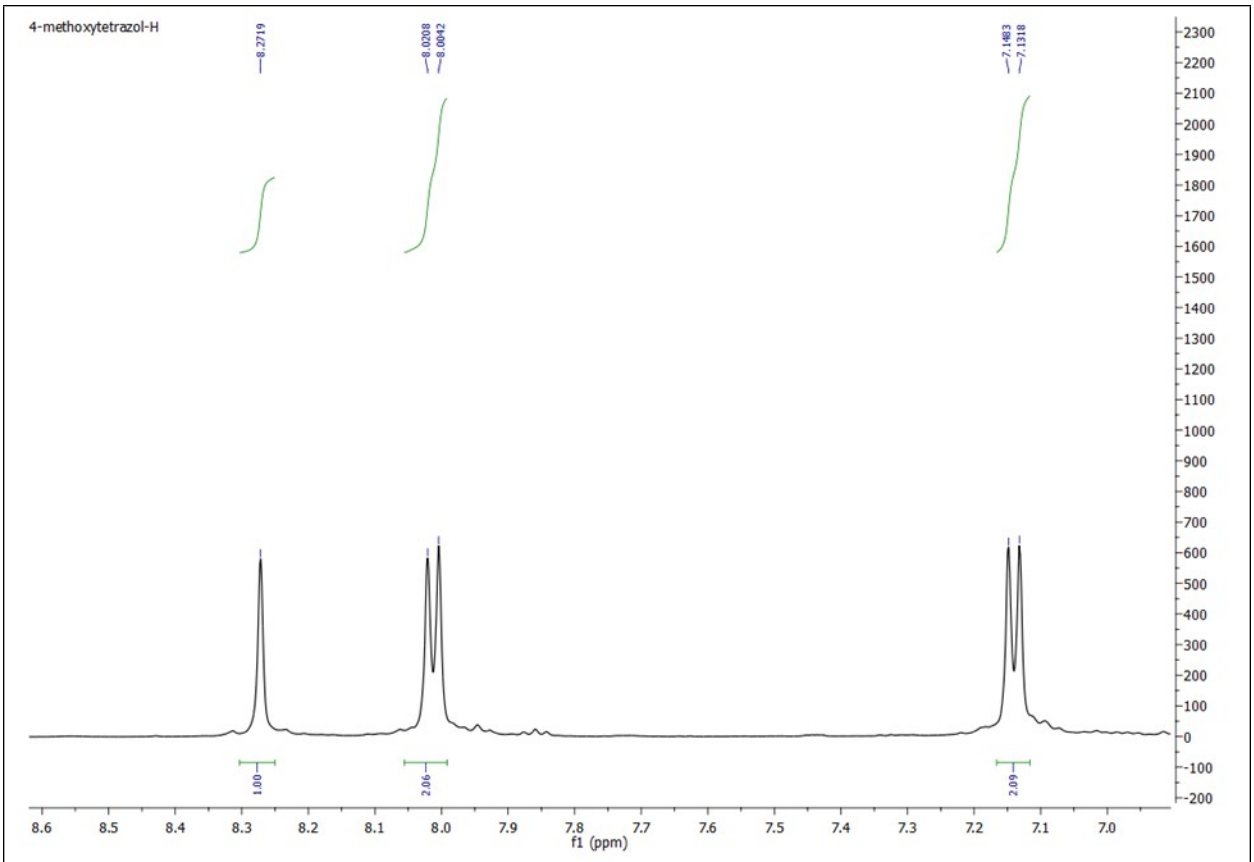

Fig. S14 Expanded ^{1}H NMR spectrum of (*E*)-3-(4-methoxyphenyl)-2-(1*H*-tetrazole-5-yl) acrylonitrile (**5l**).

(*E*)-3-(4-methylphenyl)-2-(1*H*-tetrazole-5-yl) acrylonitrile (5n):
Cream solid powder; Mp: 189-191 °C; FT-IR (KBr) ν: 3029, 2217, 1575, 1556, 1376, 1217, 1174, 813, 609 cm^{-1}; ^{1}H NMR (500 MHz, DMSO-d_6): δ (ppm) 7.41-7.43 (d, *J* =8.0 Hz, 2H), 7.92-7.94 (d, *J* = 8.0 Hz, 2H), 8.34 (s, 1H, CH), 13.40 (s, 1H, NH).

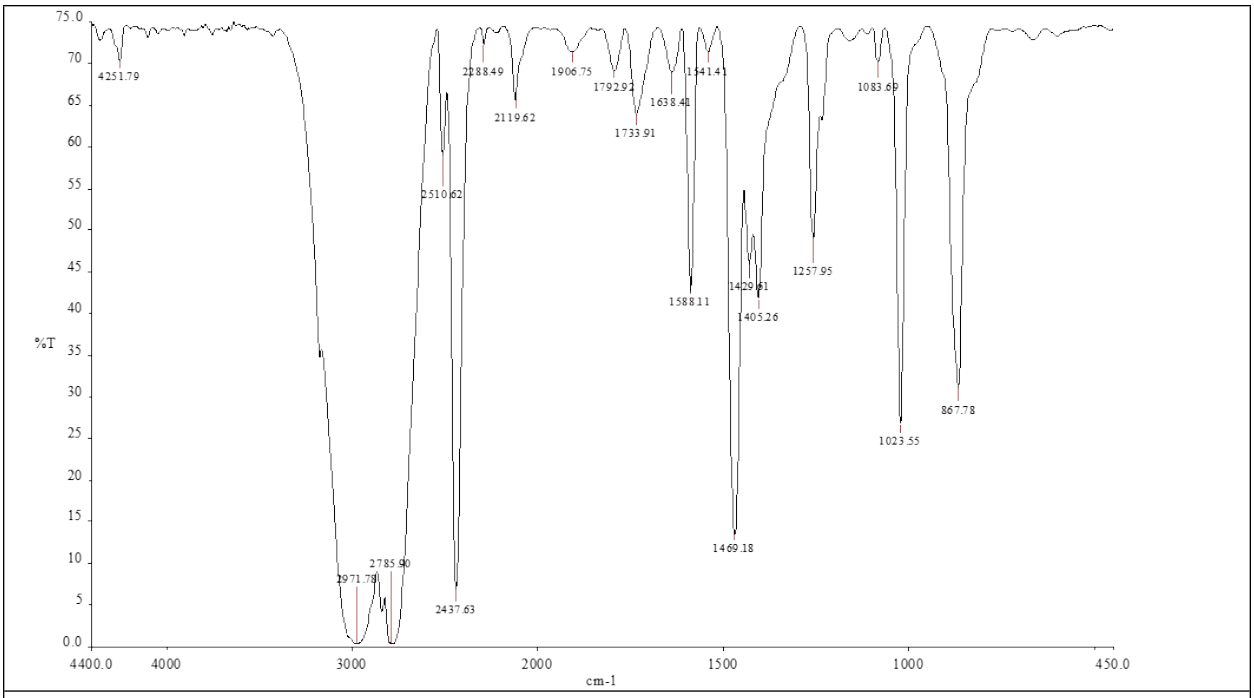

Fig. S15 FT-IR spectrum of (*E*)-3-(4-Methylphenyl)-2-(1*H*-tetrazole-5-yl) acrylonitrile (**5n**).

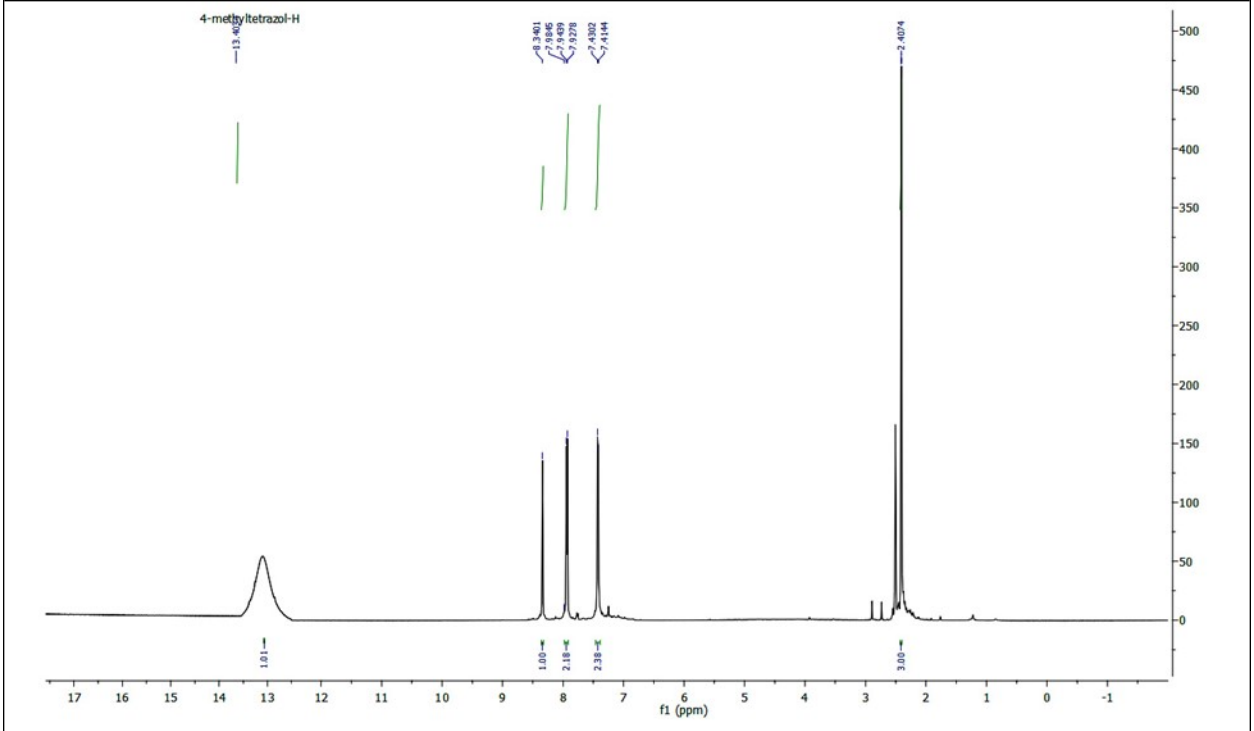

Fig. S16 ^{1}H NMR spectrum of (*E*)-3-(4-Methylphenyl)-2-(1*H*-tetrazole-5-yl) acrylonitrile (**5n**).

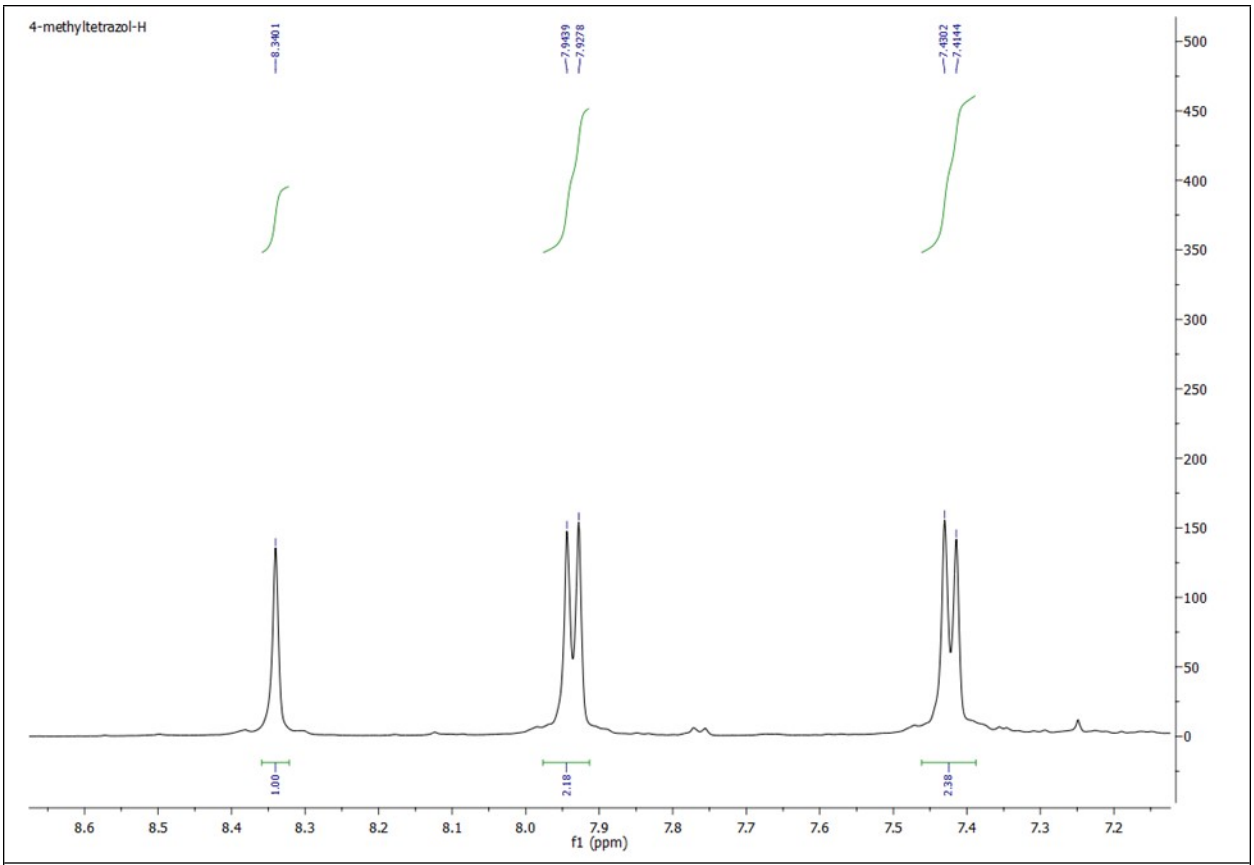

Fig. S17 Expanded ^{1}H NMR spectrum of (*E*)-3-(4-methylphenyl)-2-(1*H*-tetrazole-5-yl) acrylonitrile (**5n**).